IEEE Access
Multidisciplinary ⋮ Rapid Review ⋮ Open Access Journal

Received March 9, 2022, accepted March 24, 2022, date of publication April 5, 2022, date of current version June 14, 2022.

Digital Object Identifier 10.1109/ACCESS.2022.3165038

Large Direction-of-Arrival Mismatch Correction for Adaptive Beamforming

LIN CHANG[1], HUA YANG[1], T. AARON GULLIVER[2], (Senior Member, IEEE), SHIZHE TAN[1], AND YAN WANG[3]

[1]Department of Electrical Engineering, Ocean University of China, Qingdao 266100, China
[2]Department of Electrical and Computer Engineering, University of Victoria, Victoria, BC V8W 2Y2, Canada
[3]Department of Physics and Electronic Engineering, Taishan University, Tai'an 271000, China

Corresponding author: Shizhe Tan (tanshizhe@ouc.edu.cn)

This work was supported in part by the National Natural Science Foundation of China under Grant 91938204, Grant 41527901, and Grant 61701462; in part by the Marine S&T Fund of Shandong Province for Pilot National Laboratory for Marine Science and Technology (Qingdao) under Grant 2018SDKJ0210; in part by the Open Studio for Marine High Frequency Communications; and in part by the Scientific Research Startup Foundation of Taishan University under Grant Y-01-2020016.

ABSTRACT Direction-of-arrival (DOA) mismatch can degrade the performance of adaptive beamforming algorithms. Thus, a projection method is proposed to correct this mismatch. In a beamforming algorithm, the DOA error is usually regarded as a steering vector error which is corrected using a steering vector optimization algorithm. This approach can provide an optimal steering vector but ignores the actual DOA estimate. The proposed algorithm provides correction after DOA estimation but before beamforming to improve both the DOA estimation accuracy and beamforming gain. First, the signal-to-noise ratio (SNR) of the signal is estimated and used to regularize the covariance matrix. Then, an estimated steering vector with DOA close to the true value is determined based on a minimum number of projections. Numerical results are presented to verify the effectiveness of the proposed method for DOA estimation correction. In most cases, this method improves the performance of the beamforming algorithms without changing them.

INDEX TERMS Direction-of-arrival (DOA) mismatch correction, adaptive beamforming, covariance matrix regularization, projection method.

I. INTRODUCTION

Adaptive beamforming is an important technique in array signal processing. It has been widely applied in radar [1], sonar [2], wireless communication [3], microphone array speech signal processing [4], medical imaging [5], and radio astronomy [6]. Compared with traditional beamforming which does not depend on the received data, adaptive beamforming optimizes the weight vector based on the received data and an optimality criterion. Moreover, this vector can be adjusted according to the environment to suppress both noise and interference. However, errors exist in practical antenna arrays due to the effect of the signal-of-interest (SOI) on the training data and a small number of snapshots can severely degrade performance. Several adaptive beamforming algorithms have been proposed to solve these problems including diagonal loading [7]–[9], eigenspace projection [10]–[12], uncertainty constraint [13], [14], steering vector estimation [15]–[18], covariance matrix reconstruction [19]–[21], and a combination of the latter two [22]–[24].

Diagonal loading is a simple robust adaptive beamforming (RAB) method that has low computational complexity. However, it is difficult to choose an appropriate loading level. To deal with this issue, some schemes select the loading level automatically [25], [26]. Low computational complexity and simplicity make eigenspace projection methods popular for real-time applications. While they can deal with arbitrary errors in the steering vector, the number of subspaces can impact performance. Further, the performance is poor when the SNR is low. Uncertainty set constraint beamformers such as worst-case (WC) [13] can solve the problems with eigenspace projection methods, but the performance is degraded at high SNRs. Combined methods which employ steering vector estimation and covariance matrix reconstruction can be employed to overcome these issues. They are robust to many types of array errors and effective over a wide SNR range, but the computational complexity

The associate editor coordinating the review of this manuscript and approving it for publication was Hasan S. Mir.

This work is licensed under a Creative Commons Attribution 4.0 License. For more information, see https://creativecommons.org/licenses/by/4.0/

is high. Thus, there is a tradeoff between complexity and performance.

Steering vector estimation algorithms [18] require an initial SOI estimate. With the approaches in [19], [20], the steering vector of the interference signal is needed a priori to reconstruct the interference-plus-noise covariance (INC) matrix. The DOA is required to form the steering vector, and this can be determined using a DOA estimation algorithm or approximate orientation prediction. However, a large DOA mismatch in the received signal will result in significant errors in the steering vector [18], [23]. This will also make it difficult to determine the INC matrix [19], resulting in performance degradation. Conventional algorithms such as multiple signal classification (MUSIC) [27] and Capon [28] are commonly used in DOA estimation, but the estimation performance is poor when the SNR is low and with gain-phase uncertainties. Several techniques have been proposed to improve the performance of these algorithms such as sparse array configurations [29], DOA estimation with uncertain gain-phase sensors [30], and modified MUSIC algorithms [31].

To reduce DOA mismatch and make beamforming more robust, the DOA is corrected in this paper based on a minimum number of projections of the steering vector in the observation region. The received signal characteristics when the SNR is low and high differ. Thus, an SNR estimation algorithm is designed to distinguish between low and high SNRs. Since the noise level is large when the SNR is low, the influence of noise should be reduced in this case by adjusting the signal covariance matrix. One approach employs a tridiagonal matrix, but this requires selecting an appropriate loading level. Therefore, we combine the estimated SNR with the desired signal steering vector and signal covariance matrix to adaptively determine this level. In beamforming algorithms, the DOA error is usually regarded as a steering vector error which is corrected by a steering vector optimization algorithm. Here, a modified DOA is determined based on the minimum number of projections of a presumed steering vector onto the eigenvalues of the modified covariance matrix. This requires only the received signal, the array geometry, and the approximate DOA or angular sector of the desired signal. This method can improve beamforming performance in most cases by correcting the DOA mismatch without changing the algorithm.

The rest of this paper is organized as follows. Section 2 presents the background and introduces the signal model for adaptive beamforming. The proposed method is given in Section 3. Numerical results are presented and discussed in Section 4, and finally some conclusions are given in Section 5.

II. SIGNAL MODEL AND BACKGROUND

Consider a uniform linear array (ULA) composed of M omnidirectional sensors that receive N uncorrelated narrowband signals from far-field sources. These N signals consist of one SOI and $N-1$ interference signals impinging on the array from directions $\theta_1, \ldots, \theta_N$, respectively. The length M received signal vector at time k can be expressed as

$$\mathbf{x}(k) = \mathbf{x}_s(k) + \mathbf{x}_i(k) + \mathbf{x}_n(k) \tag{1}$$

where $\mathbf{x}_s(k) = s_1(k)\mathbf{a}_1$, $\mathbf{x}_i(k) = \sum_{j=2}^{N} s_j(k)\mathbf{a}_j$ and $\mathbf{x}_n(k)$ are the desired signal, interference and noise, respectively. The desired signal waveform is $s_1(k)$ and the corresponding steering vector is $\mathbf{a}_1$. The interference signal waveforms are $s_j(k), j = 2, 3, \ldots, N$ and the corresponding steering vectors are $\mathbf{a}_j$. $\mathbf{x}_n(k)$ is complex white Gaussian noise with zero mean and variance σ_n^2.

The steering vector of the array can be formulated as

$$\mathbf{a}(\theta) = [1, \mathrm{e}^{-j2\pi d \sin\theta/\lambda}, \ldots, \mathrm{e}^{-j2\pi(M-1)d\sin\theta/\lambda}]^T \tag{2}$$

where $(\cdot)^T$ denotes transpose, λ is the carrier wavelength, d is the distance between adjacent sensors, and the signal angle is θ. The output of the beamformer at time k can be expressed as

$$y(k) = \mathbf{w}^H \mathbf{x}(k) \tag{3}$$

where $(\cdot)^H$ denotes Hermitian transpose and $\mathbf{w} = [w_1, w_2, \ldots, w_M]^T$ is the complex weight vector. The optimal weight vector can be obtained by maximizing the output signal-to-interference-plus-noise ratio (SINR) which is defined as

$$SINR = \frac{\sigma_1^2 \left|\mathbf{w}^H \mathbf{a}_1\right|^2}{\mathbf{w}^H \mathbf{R}_{in} \mathbf{w}} \tag{4}$$

where σ_1^2 is the power of the desired signal and $\mathbf{R}_{in}$ is the INC matrix given by

$$\begin{aligned}\mathbf{R}_{in} &= E\{(\mathbf{x}_i(k) + \mathbf{x}_n(k))(\mathbf{x}_i(k) + \mathbf{x}_n(k))^H\} \\ &= \sum_{j=2}^{N} \sigma_j^2 \mathbf{a}_j \mathbf{a}_j^H + \sigma_n^2 \mathbf{I}_M\end{aligned} \tag{5}$$

σ_j^2 and σ_n^2 are the power of the jth interference signal and noise, respectively, $E\{\cdot\}$ denotes statistical expectation, and $\mathbf{I}_M$ is the $M \times M$ identity matrix.

The SINR in (4) can be maximized by minimizing the output interference-plus-noise power. Thus, the weight vector optimization problem is

$$\min_{w} \mathbf{w}^H \mathbf{R}_{in} \mathbf{w} \quad \text{s.t. } \mathbf{w}^H \mathbf{a}_1 = 1 \tag{6}$$

known as the minimum variance distortionless response (MVDR) beamformer. The corresponding solution is given by

$$\mathbf{w} = \frac{\mathbf{R}_{in}^{-1} \mathbf{a}_1}{\mathbf{a}_1{}^H \mathbf{R}_{in}^{-1} \mathbf{a}_1} \tag{7}$$

The total received signal covariance matrix $\mathbf{R}$ is usually used instead of $\mathbf{R}_{in}$ because an estimate of $\mathbf{R}_{in}$ is difficult to obtain in practice. $\mathbf{R}$ can be expressed as

$$\begin{aligned}\mathbf{R} &= E\{(\mathbf{x}_s(k) + \mathbf{x}_i(k) + \mathbf{x}_n(k))(\mathbf{x}_s(k) + \mathbf{x}_i(k) + \mathbf{x}_n(k))^H\} \\ &= \sigma_1^2 \mathbf{a}_1 \mathbf{a}_1^H + \sum_{j=2}^{N} \sigma_j^2 \mathbf{a}_j \mathbf{a}_j^H + \sigma_n^2 \mathbf{I}_M \\ &= \mathbf{R}_s + \mathbf{R}_{in}\end{aligned} \tag{8}$$

where $\mathbf{R}_s$ is the desired signal covariance matrix. The eigenvalue decomposition (EVD) of $\mathbf{R}$ is

$$\mathbf{R} = \sum_{i=1}^{M} \lambda_i \mathbf{e}_i \mathbf{e}_i^H \tag{9}$$

where $\lambda_1 \geq \lambda_2 \geq \ldots \geq \lambda_{N+1} = \ldots = \lambda_M = \sigma_n^2$ are the eigenvalues of $\mathbf{R}$, and $\mathbf{e}_i$, $i = 1, 2, \ldots, M$, are the corresponding eigenvectors. In practical applications, $\mathbf{R}$ is also unavailable and so is commonly replaced by the sample covariance matrix (SCM)

$$\hat{\mathbf{R}} = \frac{1}{K} \sum_{k=1}^{K} \mathbf{x}(k)\mathbf{x}^H(k) \tag{10}$$

where K is the number of samples. Then, the MVDR beamformer becomes the sample covariance inversion (SMI) beamformer and the corresponding weight vector is

$$\mathbf{w}_{SMI} = \frac{\hat{\mathbf{R}}^{-1}\mathbf{a}_1}{\mathbf{a}_1{}^H \hat{\mathbf{R}}^{-1}\mathbf{a}_1} \tag{11}$$

III. PROPOSED METHOD

A. DIRECTION-OF-ARRIVAL CORRECTION

DOA estimation mismatch will affect the steering vector according in (2). Further, if the beamformer weight vector $\mathbf{w}$ is obtained using (7) or (11), SOI steering vector mismatch will affect this weight vector. Moreover, if the reconstruction of $\mathbf{R}_{in}$ in (7) requires the interference steering vectors, then DOA mismatch of the interference signals will also influence $\mathbf{w}$. In this section, an algorithm is introduced for DOA mismatch correction (DC).

The goal of DC is to determine the most suitable steering vector using the projection of each steering vector on the eigenvectors in the observation region. From [32], the mismatch between the actual steering vector $\mathbf{a}$ and the presumed steering vector $\bar{\mathbf{a}}$ is small. Thus, the eigenvectors related to the projection of $\bar{\mathbf{a}}$ on the eigenvectors $\mathbf{e}_i$ can be used to construct the desired signal subspace. This projection can be represented as

$$p_i = \left|\mathbf{e}_i{}^H \bar{\mathbf{a}}\right|^2 \quad i = 1, 2, \ldots, M \tag{12}$$

Now rearrange the p_i in descending order so that $\dot{p}_{[M]} \geq \dot{p}_{[M-1]} \geq \ldots \geq \dot{p}_{[1]}$ where $\dot{p}_{[M]}$ denotes the largest of p_i values and $\dot{p}_{[1]}$ denotes the smallest. Then, the corresponding eigenvectors are $\dot{\mathbf{e}}_{[M]}, \dot{\mathbf{e}}_{[M-1]}, \ldots, \dot{\mathbf{e}}_{[1]}$. From [18], [32], if

$$\frac{\dot{p}_{[M]} + \dot{p}_{[M-1]} + \cdots + \dot{p}_{[m]}}{\sum_{i=1}^{M} p_i} > \rho \tag{13}$$

then the eigenvectors $[\dot{\mathbf{e}}_{[M]}, \dot{\mathbf{e}}_{[M-1]}, \ldots, \dot{\mathbf{e}}_{[m]}]$ span a new estimated desired signal subspace where $\sum_{i=1}^{M} p_i = M$, $0 < \rho < 1$ is the energy threshold, and m is the largest value such that (13) is satisfied.

Different from [18], [32], the purpose of the proposed DC method is not to find the desired signal subspace, but to find the minimum number of projections, i.e. the maximum value of m, that satisfies (13) in a given angle interval. In theory, $\mathbf{a}$ and $\mathbf{e}_i$ are orthogonal for $i = N+1, \ldots, M$, $\left|\mathbf{e}_i{}^H \mathbf{a}\right|^2 = 0$, so $\left|\mathbf{e}_i{}^H \bar{\mathbf{a}}\right|^2 = 0$ if $\bar{\mathbf{a}}$ is equal to $\mathbf{a}$, i.e. $p_i = 0$ for $i = N+1, \ldots, M$ and $p_i > 0$ for $i = 1, \ldots, N$. The closer $\bar{\mathbf{a}}$ is to $\mathbf{a}$, the more p_i are zero and the fewer p_i are nonzero. Since the sum of the p_i is constant, an increase in the number of nonzero p_i will reduce their average value, so the number of elements required in the numerator to satisfy (13) will also increase when ρ is properly valued. Thus, considering only look direction error, different signal angles θ will result in different $\bar{\mathbf{a}}$ and each will have a corresponding value of m. When there is no look direction error ($\bar{\mathbf{a}} = \mathbf{a}$), let $\dot{p}_{[M]} + \dot{p}_{[M-1]} + \cdots + \dot{p}_{[m_1]} / \sum_{i=1}^{M} p_i > \rho$. Then, if there is a look direction error ($\bar{\mathbf{a}} \neq \mathbf{a}$), for an m_2 that satisfies $\dot{p}_{[M]} + \dot{p}_{[M-1]} + \cdots + \dot{p}_{[m_2]} / \sum_{i=1}^{M} p_i > \rho$, it can be concluded that $m_1 \geq m_2$. Therefore, for θ located in the angular sector Θ_s of the desired signal, the θ corresponding to the maximum value of m, m_{max}, can be considered to reconstruct the steering vector. In practice, $\mathbf{R}$ is replaced by $\hat{\mathbf{R}}$, $\mathbf{e}_i$ is derived from the EVD of $\hat{\mathbf{R}}$ and $\left|\mathbf{e}_i{}^H \mathbf{a}\right|^2 \neq 0$ for $i = N+1, \ldots, M$. Since the value of $\left|\mathbf{e}_i{}^H \mathbf{a}\right|^2$ is small for $i = N+1, \ldots, M$, the proposed DC method is still applicable.

Fig. 1 presents the average value of m versus the estimated angle θ without mismatch when the true DOA is 5° for 500 Monte Carlo trials and $K = 30$. Some values of m appear as non-integers because it is the average of 500 trials, and m are integers in each trial. It is assumed that the signal angular sector is $\Theta_s = [\bar{\theta} - 5°, \bar{\theta} + 5°]$ with angle interval 0.5° where $\bar{\theta} = 5°$ is the presumed DOA and $\theta \in \Theta_s$. These results show that the value of m increases as θ approaches the true DOA, and the maximum value of m is not unique when θ is near the real DOA. The projection in (12) can be rewritten as

$$p_i = \left|\mathbf{e}_i{}^H \mathbf{d}(\theta)\right|^2 \tag{14}$$

where $\mathbf{d}(\theta)$ is the steering vector corresponding to θ and θ is located in the angular sector Θ_s of the desired signal. m_{max} is obtained by substituting θ in (14) and determining the corresponding largest value of m satisfying (13).

In practice, the modified DOA $\hat{\theta}$ can be obtained by averaging $\theta_{\min}$ and $\theta_{\max}$

$$\hat{\theta} = (\theta_{\min}(m_{\max}) + \theta_{\max}(m_{\max}))/2 \tag{15}$$

where $\theta_{\min}$ is the minimum angle for which m is maximum and $\theta_{\max}$ is the maximum angle for which m is maximum. If there is only one maximum for m in Θ_s, then $\hat{\theta} = \theta_{\min} = \theta_{\max}$. For an input SNR of −20 dB, −10 dB, 0 dB, 10 dB, and 20 dB, Fig. 1 indicates that the value of $\hat{\theta}$ estimated using the DC method is 2.5°, 4°, 4.5°, 5°, and 5°, respectively.

Fig. 2 shows the average value of m versus the estimated DOA angle θ when the direction mismatch is uniformly distributed in [−4°, 4°] when the true DOA is 5° (so $\bar{\theta}$ is uniformly distributed in [1°, 9°]), for 500 Monte Carlo trials. For input SNR values −20, −10, 0, 10 and 20 dB, $\hat{\theta}$ is 3.5°, 4.75°, 5°, 4.5°, and 5°, respectively. The root-mean-square-error (RMSE) of the DOA estimates with and without the DC

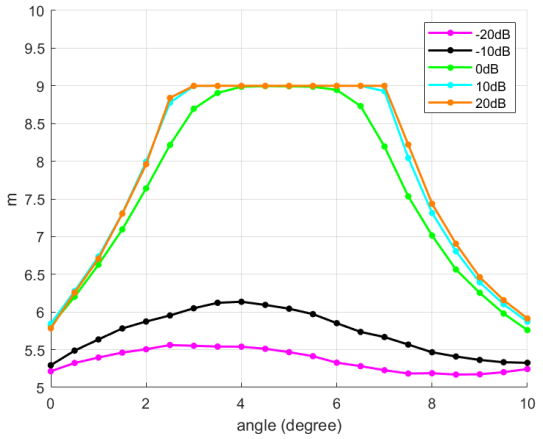

FIGURE 1. Average *m* versus the estimated angle for 500 Monte Carlo trials.

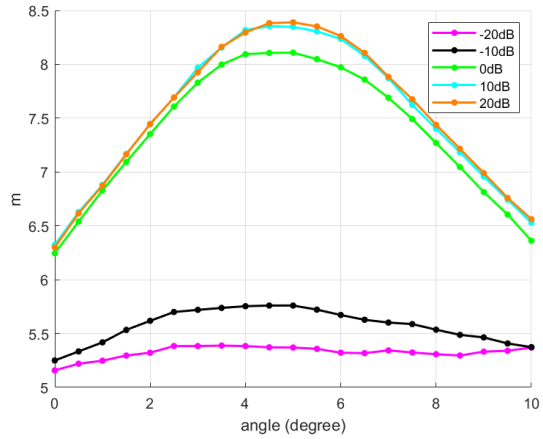

FIGURE 2. Average *m* versus the estimated angle with DOA mismatch for 500 Monte Carlo trials.

method versus SNR is shown in Fig. 3 with $K = 30$ and look direction mismatch uniformly distributed in $[-4°, 4°]$ for 500 Monte Carlo trials. Figs. 1, 2, and 3 show that the DC method can reduce the DOA estimation mismatch when the SNR is high but large errors still exist when the SNR is low. Thus, an algorithm for low input SNR is developed in the next section.

B. MODIFIED COVARIANCE MATRIX

Figs. 1, 2, and 3 show that the DOA estimation error increases as the SNR decreases. This performance degradation is mainly due to noise. In order to reduce the influence of noise when the SNR is low, the SNR of the desired signal must first be estimated. The input SNR of the received signal can be estimated as

$$SNR_{input} = 10\log_{10}\sigma_1^2/\sigma_n^2 \tag{16}$$

Note that both σ_1^2 and σ_n^2 are unknown. Thus, the SNR is approximated as

$$SNR_{approx} = 10\log_{10}0.1\dot{\lambda}_{[M]}/\bar{\sigma}_n^2 \tag{17}$$

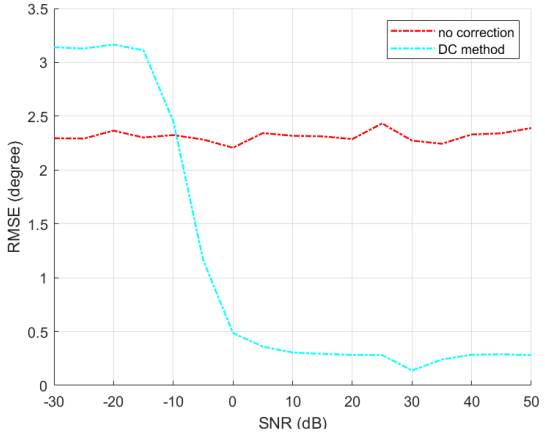

FIGURE 3. RMSE of the DOA estimates versus input SNR with direction mismatch.

The estimated noise power is then

$$\bar{\sigma}_n^2 = \frac{1}{M-N}\sum_{i=N+1}^{M}\lambda_i \tag{18}$$

The input SNR is considered low if $SNR_{approx} < 0$. Define $\beta = 0.1\dot{\lambda}_{[M]}/\bar{\sigma}_n^2$ where $\dot{\lambda}_{[M]}$ is the eignevalue corresponding to the eigenvector $\dot{\mathbf{e}}_{[M]}$ obtained from $\left|\dot{\mathbf{e}}_{[M]}^H\bar{\mathbf{a}}\right|^2 = \dot{p}_{[M]}$. This expression was determined based on extensive simulations. In this paper, a tridiagonal loading algorithm is used to reduce the DOA estimation mismatch when the input SNR is low. This is an effective way to mitigate beamforming issues caused by noise and/or model errors [33]. The loaded SCM can be expressed as

$$\hat{\mathbf{R}}_L = \hat{\mathbf{R}} + \tau\mathbf{T} \tag{19}$$

where τ is the loading level and the loading matrix $\mathbf{T}$ is a simple tridiagonal Toeplitz matrix given by

$$\mathbf{T} = \begin{bmatrix} 1 & -2 & 0 & \cdots & 1 & 1 \\ -2 & 1 & -2 & \cdots & 0 & 1 \\ 0 & -2 & 1 & \cdots & 0 & 0 \\ \vdots & \vdots & \vdots & \ddots & \vdots & \vdots \\ 1 & 0 & 0 & \cdots & 1 & -2 \\ 1 & 1 & 0 & \cdots & -2 & 1 \end{bmatrix} \tag{20}$$

The loading level in (19) is given by

$$\tau = (\|\tilde{\mathbf{a}}\|)^{-1}\tilde{\mathbf{a}}^H\hat{\mathbf{R}}\tilde{\mathbf{a}} \tag{21}$$

where the weighted steering vector is

$$\tilde{\mathbf{a}} = \beta \odot \bar{\mathbf{a}} \tag{22}$$

and $\odot$ denotes componentwise product. The modified sample covariance matrix can be expressed as

$$\mathbf{R}_c = \begin{cases} \hat{\mathbf{R}}, & \beta \geq 1 \\ \hat{\mathbf{R}}_L, & \beta < 1 \end{cases} \tag{23}$$

The proposed DOA correction algorithm is given in Algorithm 1. The complexity of this algorithm is $\mathcal{O}(M^3)$.

Algorithm 1 Proposed DOA Correction Algorithm

Step 1: Estimate the sample covariance matrix $\hat{\mathbf{R}}$ using (10).
Step 2: Eigen-decompose $\hat{\mathbf{R}}$ to get the eigenvalues λ_i and eigenvectors $\mathbf{e}_i$.
Step 3: Compute p_i in (12), find the maximum value $\dot{p}_{[M]}$ in p_i to get the eigenvector $\dot{\mathbf{e}}_{[M]}$ and the corresponding eigenvalue $\dot{\lambda}_{[M]}$.
Step 4: Let $\beta = 0.1\dot{\lambda}_{[M]}/\bar{\sigma}_n^2$ and adjust $\mathbf{R}_c$ according to (23).
Step 5: Eigen-decompose $\mathbf{R}_c$ to get the new eigenvectors $\mathbf{e}_i$, substitute θ in (14) in sequence within the angular sector Θ_s to obtain the p_i, calculate the corresponding m using (13).
Step 6: Find m_{max} and determine $\hat{\theta}$ from Θ_s using (15).

IV. PERFORMANCE EVALUATION

In this section, numerical results are presented to validate the effectiveness of the proposed method. Consider a uniform linear array with $M = 10$ omnidirectional sensors spaced half a wavelength apart. The noise is modeled as complex Gaussian which is temporally and spatially white with zero mean and unit covariance. Each result is the average of 500 Monte-Carlo trials.

A. DOA ESTIMATION PERFORMANCE

1) DOA CORRECTION WITH RANDOM LOOK DIRECTION ERRORS

The performance with large DOA errors is now considered. The desired signal impinges on the array from the direction $\theta_1 = 5°$, and the direction mismatch is randomly and uniformly distributed in [−4°,4°]. Fig. 4 presents the RMSE of the DOA estimate versus SNR for $K = 30$. The red dotted line is the RMSE with no correction, the blue dotted line is the RMSE with correction using the DC method, and the solid green line is the RMSE with correction using the proposed method. This shows that the proposed algorithm effectively corrects the DOA error even at low SNRs. Fig. 5 presents the RMSE versus the number of snapshots for an input SNR of 20 dB (high SNR). This shows that the number of snapshots has a negligible effect on the RMSE. Note that for a high SNR, $\mathbf{R}_c$ in the DC method is the same as that in the proposed method, so the blue dotted and solid green lines coincide.

2) RMSE PERFORMANCE

DOA estimation algorithms with the proposed method are now examined. The RMSE differences with and without the proposed method are used to evaluate the performance. The MUSIC and Capon DOA estimation methods as well as the rational invariance (ESmusic) [34], propagator method (PM) [35], modified propagator method (MPM) [36], and DOA estimation with uncertain gain-phase sensors (DSS) [30] techniques are considered. The desired signal impinges on the array from the direction $\theta_1 = 5°$.

Fig. 6 presents the RMSE of the DOA estimation algorithms versus the input SNR under ideal conditions with $K = 30$, and Fig. 7 gives the corresponding RMSE versus the number of snapshots under ideal conditions with SNR $= -10$ dB.

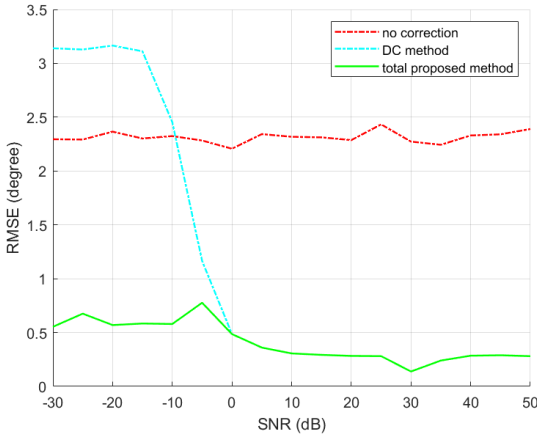

FIGURE 4. DOA estimation RMSE versus input SNR.

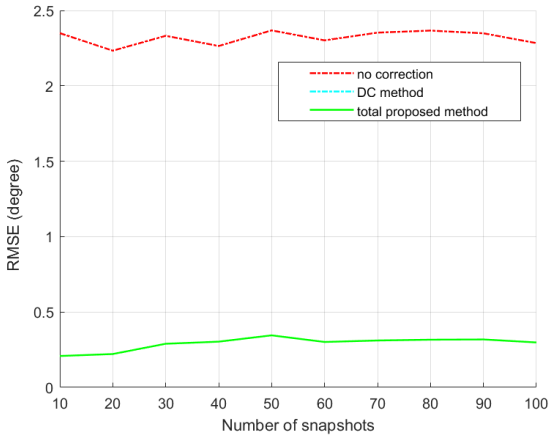

FIGURE 5. DOA estimation RMSE versus the number of snapshots.

TABLE 1. Angle sectors for different SNRs.

Input SNR (dB)	Angle sector	Angle interval
$[-15,-5]$	$[\theta_1-5°,\theta_1+5°]$	1°
$[-5,0]$	$[\theta_1-2°,\theta_1+2°]$	0.2°
$[0,10]$	$[\theta_1-1°,\theta_1+1°]$	0.1°
$[10,15]$	$[\theta_1-0.5°,\theta_1+0.5°]$	0.05°

These results show that the RMSE is large at low SNRs and small at high SNRs, so the angle range considered should be based on the SNR. As a consequence, the signal angle sector is set according to the input SNR as shown in Table 1. Taking the second row as an example, when the input SNR is between $[-15, -5]$, the angle sector is $\Theta_s = [\theta_1 - 5°, \theta_1 + 5°]$ with angle interval 1°.

The RMSE difference is shown in Fig. 8 versus the SNR. A difference less than 0 indicates that the proposed method reduces the RMSE of the algorithm and makes it better. These results show that when the input SNR is less than 10 dB, the proposed method can reduce the estimation error of the Capon, ESmusic, PM, and MPM algorithms. For the MUSIC and DSS methods, this difference is slightly greater than 0 when the SNR is in the range $[-5, 5]$. When the SNR

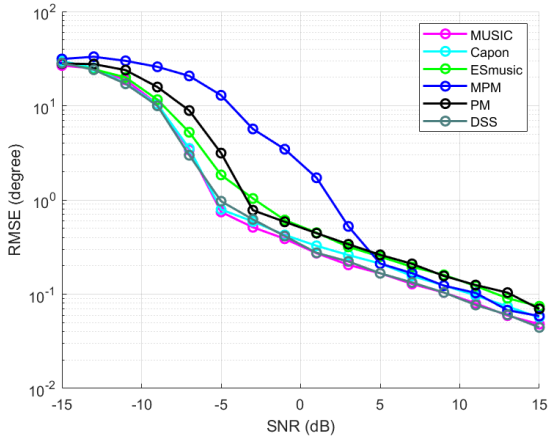

FIGURE 6. RMSE versus input SNR under ideal conditions with $K = 30$.

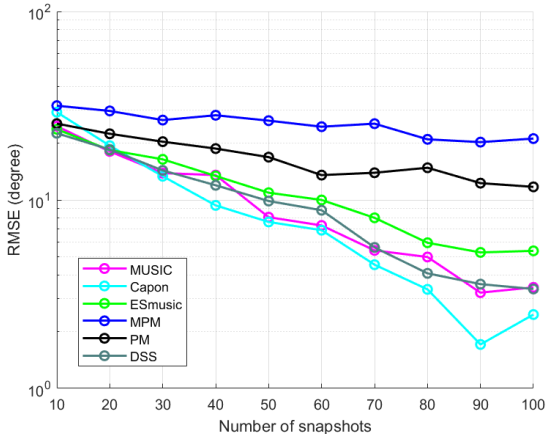

FIGURE 7. RMSE versus the number of snapshots under ideal conditions with SNR $= -10$ dB.

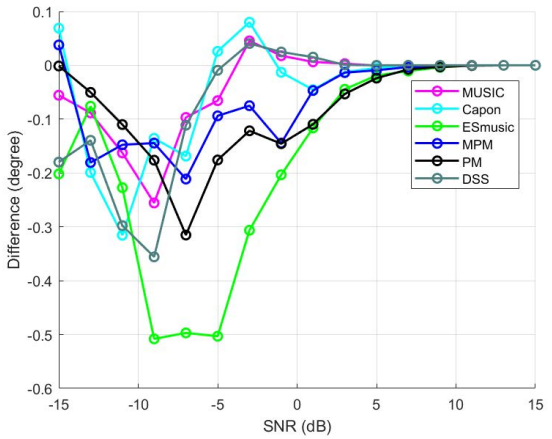

FIGURE 8. RMSE difference versus input SNR under ideal conditions with $K = 30$.

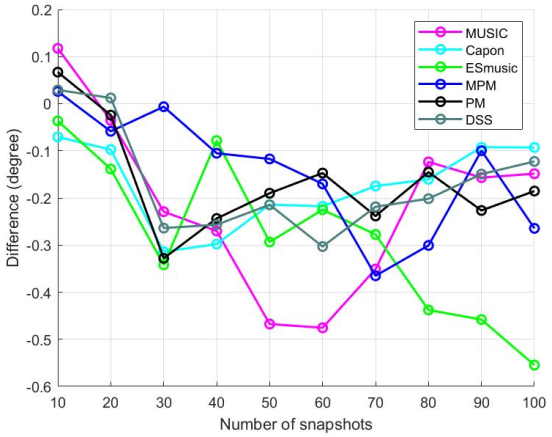

FIGURE 9. RMSE difference versus the number of snapshots under ideal conditions with SNR $= -10$ dB.

is greater than 10 dB, the effect of the proposed algorithm is small because the DOA estimation algorithms already provide accurate results. The RMSE difference versus the number of snapshots when the input SNR is -10 dB is given in Fig. 9. This shows that when the number of snapshots is greater than 20, the DOA estimation algorithms combined with the proposed method outperform the algorithms alone.

3) RMSE PERFORMANCE WITH ARRAY UNCERTAINTIES

In this section, the amplitude, phase, and sensor location errors are considered as array uncertainties. The amplitude and phase errors of each sensor are randomly distributed according to $N(0, 0.1^2)$ and $N(0, 0.25\pi^2)$, respectively, and the sensor location errors are uniformly distributed in the interval $[-0.1, 0.1]$ measured in sensor space. The nth element of the steering vector can then be expressed as

$$(1 + \Delta g)e^{-j2\pi(nd+\Delta d)\sin\theta/\lambda}e^{-j\Delta\phi}, \quad n = 0, 1, \ldots, M-1 \tag{24}$$

where Δg is the gain error, $\Delta\phi$ is the phase error, and Δd is the sensor location error. The errors were changed each trial but remain constant over the corresponding snapshots. The angle sector is chosen as previously. The RMSE difference is presented in Fig. 10. These results show that when the SNR is lower than 10 dB, the proposed algorithm can still reduce the RMSE of the original DOA estimation methods. Fig. 11 presents the RMSE difference for different numbers of snapshots. This indicates that when the number of snapshots is greater than 20, the proposed algorithm can still reduce the RMSE.

B. BEAMFORMER PERFORMANCE

In this section, the performance of the proposed method is evaluated using several beamformers widely used in the literature. One desired signal and two interference signals impinge on the array from directions $\theta_1 = 5°$, $\theta_2 = -50°$, and $\theta_3 = -20°$, respectively. The interference-to-noise ratio (INR) for both signals is set to 30 dB. The following beamforming algorithms are considered. INC matrix reconstruction and steering vector estimation (ICM) [23], INC matrix reconstruction and steering vector via subspace estimation (SICM) [22], combined INC

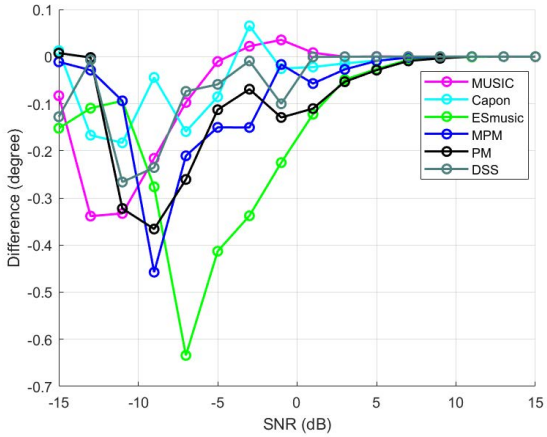

FIGURE 10. RMSE difference versus input SNR with array uncertainties and $K = 30$.

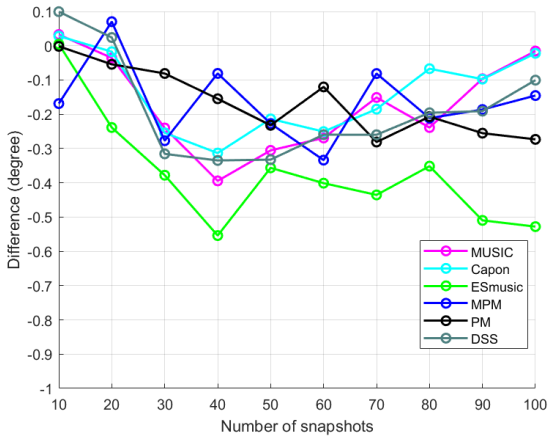

FIGURE 11. RMSE difference versus the number of snapshots with array uncertainties and SNR = −10 dB.

matrix reconstruction [19] with desired signal steering vector estimation [18] (SRNSV), worst-case-based beamformer (WC) [13], minimum sensitivity eigenspace-based beamformer (MSESB) [12], maximum entropy method (MEPS) [37], tridiagonal loading beamformer (TLBF) [33], and SMI [38]. The angle sector of the desired signal is set to $\Theta_s = [\bar{\theta} - 5°, \bar{\theta} + 5°]$ with angle interval 0.5° for the methods in [22] and [23], and the proposed method. The energy threshold for the method in [18] and the proposed method is set to $\rho = 0.9$. The number of sampling points for the MEPS method are set to $L = 50$ and $S = 10$. The weight $\mathbf{w}_{SLL}$ for the TLBF method [33] is set to 0.05, the number of dominant eigenvectors in [22] is set to 7, and ϵ in [13] is set to $0.3M$. The optimization problem is solved using CVX [39]. Fig. 12 presents the output SINR versus input SNR under ideal conditions with $K = 30$ and Fig. 13 gives the output SINR versus the number of snapshots under ideal conditions with SNR = 20 dB.

1) BEAMFORMING WITH RANDOM LOOK DIRECTION ERRORS

In this section, the influence of the proposed algorithm on the beamforming algorithms is evaluated considering signal look

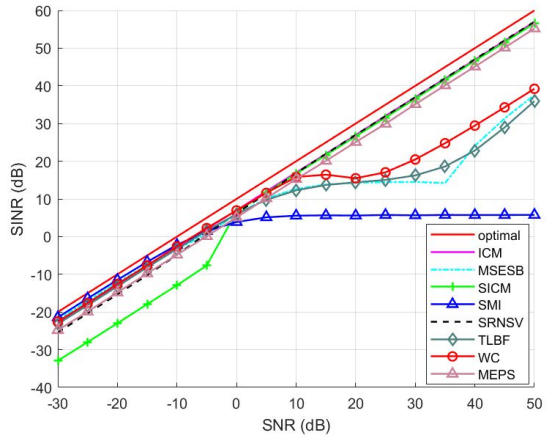

FIGURE 12. Output SINR versus input SNR under ideal conditions with $K = 30$.

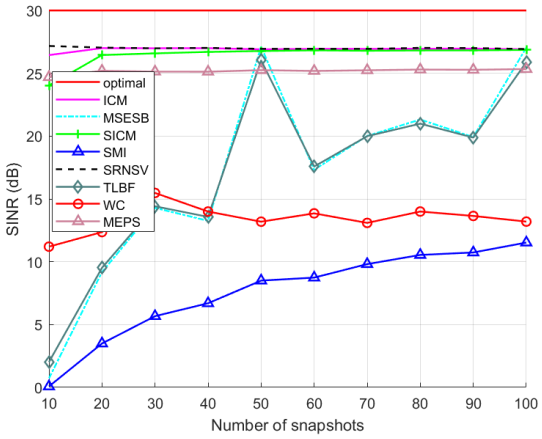

FIGURE 13. Output SINR versus the number of snapshots under ideal conditions with SNR = 20 dB.

direction errors with random direction mismatch uniformly distributed in [−4°, 4°]. Thus, the DOA estimates of the SOI and two interference signals are uniformly distributed in [1°,9°], [−54°, −46°] and [−24°, −16°], respectively. The direction errors of the three signals are changed each trial but remain constant over the corresponding snapshots. Fig. 14 presents the output SINR of the beamformers versus input SNR with $K = 30$. Comparing these results with Fig. 12 indicates that the output SINR of the beamformers decreases in the presence of look direction errors. Fig. 15 gives the output SINR difference of the beamforming algorithms with and without the proposed method versus the input SNR. These results show that the proposed method can improve beamformer performance when there are DOA estimation errors. The improvement with the SRNSV and SICM methods is significant while the improvement with the SMI and TLBF algorithms is greater when the input SNR is high.

In the SRNSV [18], [19], ICM [23], SICM [22], TLBF [33], and SMI [38] methods, $\mathbf{w}$ is obtained using (7) and the output SINR is improved with the proposed algorithm. In ICM, the estimated INC matrix is reconstructed

based on the revised SOI interval, and the steering vector optimization algorithm uses the steering vector from the proposed method. With MEPS, an improved estimate for the desired signal steering vector is obtained using the revised SOI interval. With SICM, the revised direction interval is needed to calculate the steering vector of the desired signal. In addition, the DOA of the interference signals must be estimated because the INC matrix is reconstructed based on the interference signal steering vector. Therefore, correcting the signal DOAs will improve the output SINR. The INC matrix reconstruction in SRNSV [19] requires the interference steering vector, and optimization of the steering vector of the desired signal in SRNSV [18] is based on constraints on the estimated steering vector of the desired signal. Determining these steering vectors requires the corresponding DOAs. As a result, DOA errors will affect both INC matrix reconstruction and steering vector estimation, which will decrease the output SINR. For TLBF, using the proposed method in estimating the steering vector of the desired signal and the loaded SCM regularization will improve the performance.

The performance of the SMI algorithm can be degraded when the input SNR of the desired signal is high, but using the modified $\mathbf{a}$ in (11) obtained with the proposed method can alleviate this problem. The WC algorithm is improved for input SNR in the range 0 to 30 dB, but there is minimal improvement with MSESB for all SNRs. The weight vector $\mathbf{w}$ with WC [13] beamforming is obtained based on the worst-case constraint and so is robust to steering vector errors. However, when the input SNR is in the range 0 to 30 dB, the performance of this algorithm is poor. The proposed algorithm was shown to improve this performance. With the MSESB method [12], the projection of the steering vector in the signal-interference subspace is needed to obtain $\mathbf{w}$. It is robust to steering vector errors and the subspace projection of the steering vector will reduce the effect of DOA correction. Thus, the proposed method provides little improvement for this method.

Fig. 16 presents the output SINR of the beamformers versus the number of snapshots without the proposed method for SNR $=$ 20 dB. The corresponding output SINR difference with and without the proposed method is given in Fig. 17. These results show that the proposed method improves the SINR when there are DOA estimation errors, and the improvement in SINR is greatest for the SMI and SRNSV algorithms.

2) BEAMFORMING WITH AMPLITUDE, PHASE AND SENSOR LOCATION ERRORS

In this section, the random DOA mismatch, amplitude, phase, and sensor location errors are the same as in Section IV-A3. Fig. 18 gives the output SINR difference with and without the proposed method versus the input SNR for the beamformer algorithms. These results show that the proposed algorithm improves the performance of all algorithms. SMI and TLBF are significantly improved when the SNR is high, and ICM, SICM, MEPS and SRNSV are also better. However, WC is

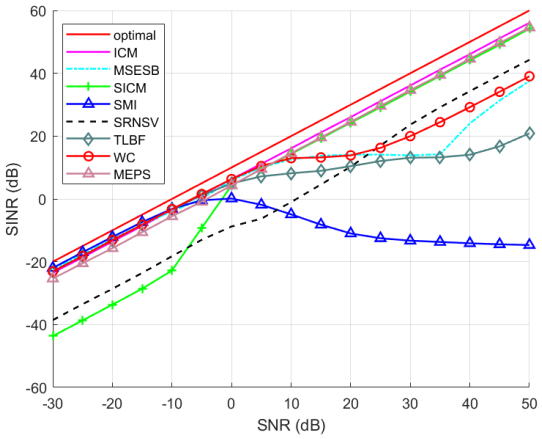

FIGURE 14. Output SINR versus input SNR with look direction errors and without the proposed method.

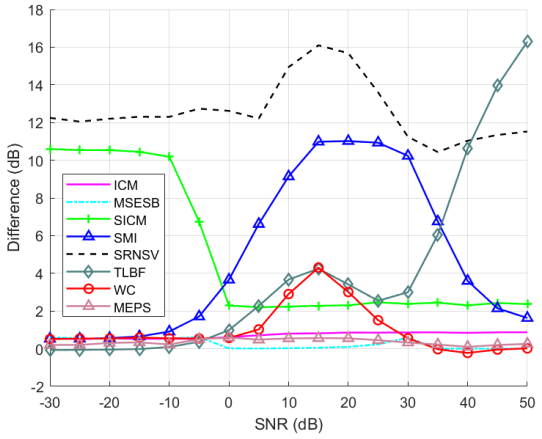

FIGURE 15. Output SINR difference versus input SNR with look direction errors.

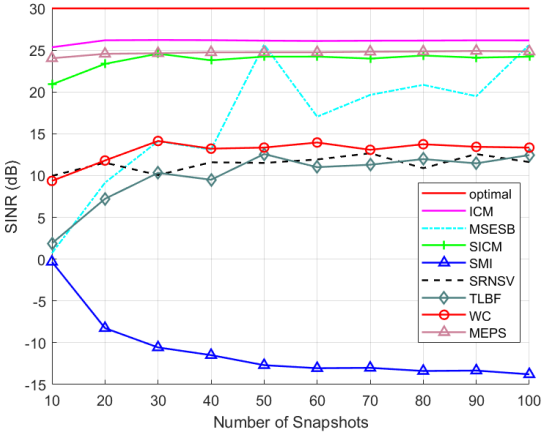

FIGURE 16. Output SINR versus the number of snapshots with look direction errors and without the proposed method.

only improved in the range SNR $=$ 0 to 30 dB, and there is little improvement for MSESB.

Fig. 19 presents the output SINR difference versus the number of snapshots for the beamformer algorithms with

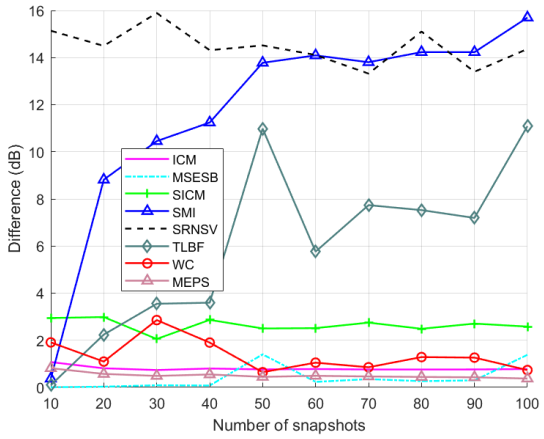

FIGURE 17. Output SINR difference versus the number of snapshots with look direction errors.

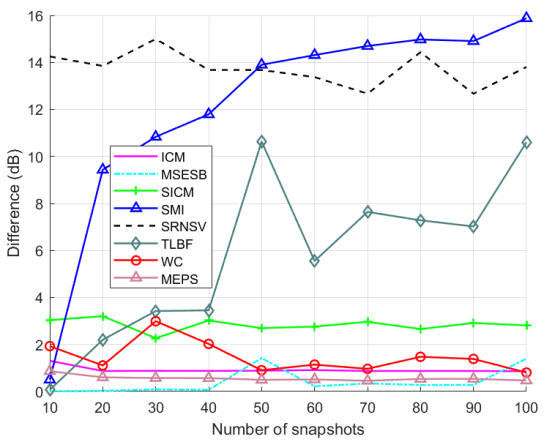

FIGURE 19. Output SINR difference versus the number of snapshots with hybrid array errors.

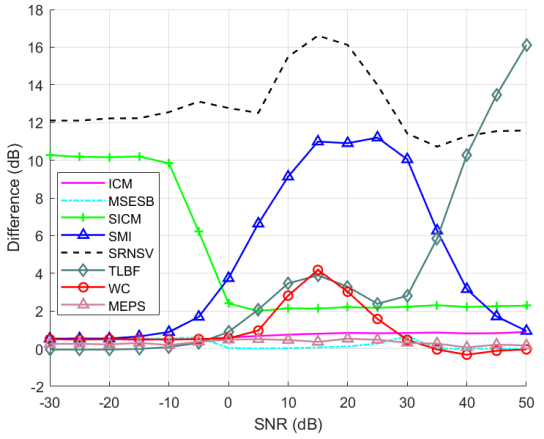

FIGURE 18. Output SINR difference versus input SNR with hybrid array errors.

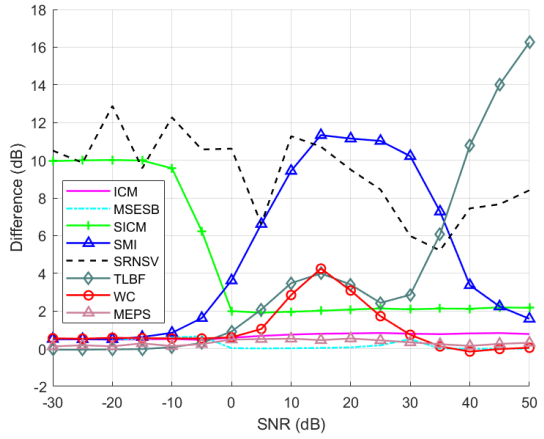

FIGURE 20. Output SINR difference versus input SNR with fast wavefront distortion.

and without the proposed method. This shows that using the proposed method improves the performance regardless of the number of snapshots. Further, these results indicate that the proposed method can improve beamforming performance with a variety of errors.

3) BEAMFORMING WITH FAST WAVEFRONT DISTORTION

In this section, the case when the signal steering vector is distorted by wave propagation is considered. Fast wavefront distortion occurs when the signal propagates in a long and inhomogeneous medium. It is assumed that the phase distortion is independent and Gaussian distributed according to $N(0, 0.1^2)$, and the distortion changes each trial and from snapshot to snapshot. The random DOA mismatch is uniformly distributed in $[-4°, 4°]$. Fig. 20 presents the output SINR difference for the beamformers with and without the proposed method versus the input SNR. This shows that the performance of the ICM, SRNSV, SMI, SICM, MEPS and TLBF algorithms with the proposed method are better over the entire SNR range, while WC is improved for SNR $=$ 0 to 35 dB. Fig. 21 gives the output SINR difference for the beamformer algorithms with and without the proposed method for different numbers of snapshots. This indicates that the output SINR of these algorithms are improved with the proposed method regardless of the number of snapshots.

4) BEAMFORMING WITH INCOHERENT LOCAL SCATTERING ERRORS

In this section, the case when the signal steering vector is affected by incoherent local scattering errors is considered. The desired signal is time-varying so the steering vector is modeled as

$$\hat{\mathbf{a}}_1(k) = s_0(k)\mathbf{a}_1 + \sum_{p=1}^{4} s_p(k)\bar{\mathbf{a}}(\theta_p) \tag{25}$$

where $s_p(k), p = 0, 1, 2, 3, 4$ are independent random variables with distribution $N(0, 1)$, and $\bar{\mathbf{a}}(\theta_p)$ are the corresponding incoherent scattering paths. The angles $\theta_p, p = 1, 2, 3, 4$ are independent random variables with distribution $N(5°, 4°)$. $s_p(k)$ changes both from trial to trial and snapshot to snapshot, the directions of arrival θ_p change from trial to trial but is constant over the corresponding snapshots.

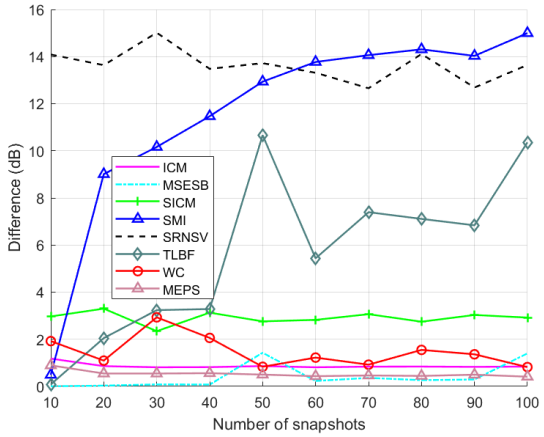

FIGURE 21. Output SINR difference versus the number of snapshots with fast wavefront distortion.

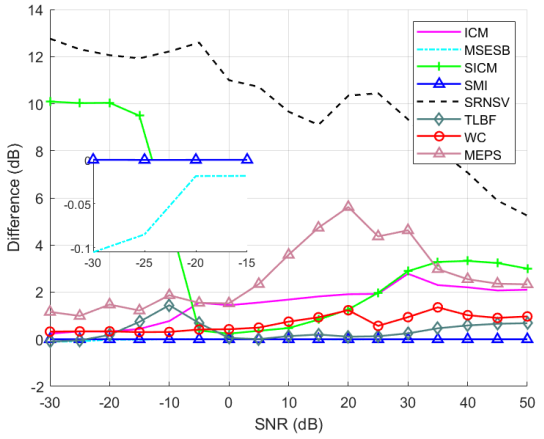

FIGURE 22. Output SINR difference versus input SNR with incoherent local scattering errors.

The random DOA mismatch is uniformly distributed in $[-4°, 4°]$. The model in (25) corresponds to the case of incoherent local scattering [40]. Under this assumption, the signal covariance matrix $\mathbf{R}_s$ is no longer a rank-one matrix and the output SINR has the form

$$SINR_{opt} = \frac{\mathbf{w}^H \mathbf{R}_s \mathbf{w}}{\mathbf{w}^H \mathbf{R}_{i+n} \mathbf{w}} \tag{26}$$

which is maximized by the weight vector [41]

$$\mathbf{w}_{opt} = \mathbb{P}\{\mathbf{R}_{i+n}^{-1} \mathbf{R}_s\} \tag{27}$$

where $\mathbb{P}\{\cdot\}$ denotes the principal eigenvector of a matrix.

Fig. 22 gives the output SINR difference for the beamformer algorithms with and without the proposed method versus the input SNR. This shows that the differences for SMI and MSESB are close to 0 dB, and the proposed method improves the output SINR of the other algorithms. Fig. 23 gives the output SINR difference for the beamformer algorithms with and without the proposed method for different numbers of snapshots. This indicates that except for SMI and MSESB, the proposed method improves the performance regardless of the number of snapshots.

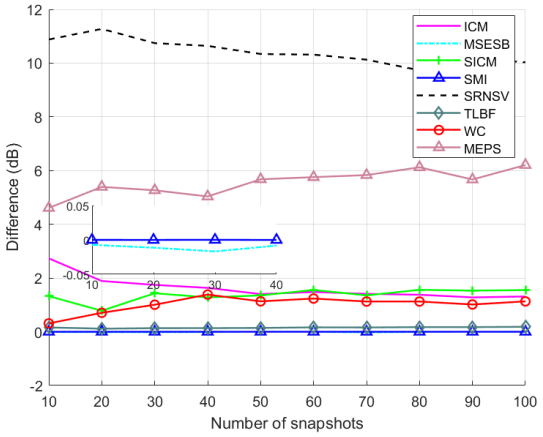

FIGURE 23. Output SINR difference versus the number of snapshots with incoherent local scattering errors.

V. CONCLUSION

In this paper, a DOA correction method was presented for array signal processing. This method provides a new approach to SNR estimation and adaptive covariance matrix modification so it can be used for a wide range of input SNRs. A modified DOA was determined based on the relationship between the eigenvectors of the covariance matrix and the actual steering vector, and this DOA can be used to construct the steering vector. The proposed approach can be utilized with any beamforming algorithm and only requires an estimated angle range for the observed signal. It can also be used after DOA estimation to correct inaccurate estimation results. Numerical results were presented which show that the proposed method can not only correct DOA estimation errors, but can cope with large DOA errors and improve the performance of beamforming algorithms which require the DOA of the signal to reconstruct the INC matrix or estimate the steering vector. Future work includes improving the robustness of the algorithm to adapt to more complex environments and employing it for signal detection.

ACKNOWLEDGMENT

The authors would like to thank Prof. Hao Zhang and his team for the experimental resources.

REFERENCES

[1] J. Xu, G. Liao, H. Lei, and H. C. So, "Robust adaptive beamforming for fast-moving target detection with FDA-STAP radar," *IEEE Trans. Signal Process.*, vol. 65, no. 4, pp. 973–984, Feb. 2017.

[2] A. E. A. Blomberg, A. Austeng, R. E. Hansen, and S. A. V. Synnes, "Improving sonar performance in shallow water using adaptive beamforming," *IEEE J. Ocean. Eng.*, vol. 38, no. 2, pp. 297–307, Apr. 2013.

[3] Z. Xiao, L. Zhu, J. Choi, P. Xia, and X. G. Xia, "Joint power allocation and beamforming for non-orthogonal multiple access (NOMA) in 5G millimeter-wave communications," *IEEE Trans. Wireless Commun.*, vol. 17, no. 5, pp. 2961–2974, May 2019.

[4] S. Gannot, E. Vincent, S. Markovich-Golan, and A. Ozerov, "A consolidated perspective on multimicrophone speech enhancement and source separation," *IEEE/ACM Trans. Audio, Speech, Language Process.*, vol. 25, no. 4, pp. 692–730, Apr. 2017.

[5] S. Khan, J. Huh, and J. C. Ye, "Adaptive and compressive beamforming using deep learning for medical ultrasound," *IEEE Trans. Ultrason., Ferroelectr., Freq. Control*, vol. 67, no. 8, pp. 1558–1572, Aug. 2020.

[6] S. W. Ellingson, "Beamforming and interference canceling with very large wideband arrays," *IEEE Trans. Antennas Propag.*, vol. 51, no. 6, pp. 1338–1346, Jun. 2003.
[7] B. D. Carlson, "Covariance matrix estimation errors and diagonal loading in adaptive arrays," *IEEE Trans. Aerosp. Electron. Syst.*, vol. 24, no. 4, pp. 397–401, Jul. 1988.
[8] A. Elnashar, S. M. Elnoubi, and H. A. El-Mikati, "Further study on robust adaptive beamforming with optimum diagonal loading," *IEEE Trans. Antennas Propag.*, vol. 54, no. 12, pp. 3647–3658, Dec. 2006.
[9] J. Zhuang, Q. Ye, Q. Tan, and A. H. Ali, "Low-complexity variable loading for robust adaptive beamforming," *Electron. Lett.*, vol. 52, no. 5, pp. 338–340, 2016.
[10] L. Chang and C.-C. Yeh, "Performance of DMI and eigenspace-based beamformers," *IEEE Trans. Antennas Propag.*, vol. 40, no. 11, pp. 1336–1347, Nov. 1992.
[11] D. D. Feldman and L. J. Griffiths, "A projection approach for robust adaptive beamforming," *IEEE Trans. Signal Process.*, vol. 42, no. 4, pp. 867–876, Apr. 1994.
[12] J. Wang, W. Zhang, and W. Liu, "Minimum sensitivity based robust beamforming with eigenspace decomposition," *Multidimensional Syst. Signal Process.*, vol. 29, no. 2, pp. 687–701, Apr. 2018.
[13] S. A. Vorobyov, A. B. Gershman, and Z.-Q. Luo, "Robust adaptive beamforming using worst-case performance optimization: A solution to the signal mismatch problem," *IEEE Trans. Signal Process.*, vol. 51, no. 2, pp. 313–324, Feb. 2003.
[14] X. Zhang, W. Liu, Y. Xu, and Z. Liu, "Quaternion-valued robust adaptive beamformer for electromagnetic vector-sensor arrays with worst-case constraint," *Signal Process.*, vol. 104, pp. 274–283, Nov. 2014.
[15] A. Khabbazibasmenj, S. A. Vorobyov, and A. Hassanien, "Robust adaptive beamforming based on steering vector estimation with as little as possible prior information," *IEEE Trans. Signal Process.*, vol. 60, no. 6, pp. 2974–2987, Jun. 2012.
[16] A. Hassanien, S. A. Vorobyov, and K. M. Wong, "Robust adaptive beamforming using sequential quadratic programming: An iterative solution to the mismatch problem," *IEEE Signal Process. Lett.*, vol. 15, pp. 733–736, 2008.
[17] Y. Huang, M. Zhou, and S. A. Vorobyov, "New designs on MVDR robust adaptive beamforming based on optimal steering vector estimation," *IEEE Trans. Signal Process.*, vol. 67, no. 14, pp. 3624–3638, Jul. 2019.
[18] W. Jia, W. Jin, S. Zhou, and M. Yao, "Robust adaptive beamforming based on a new steering vector estimation algorithm," *Signal Process.*, vol. 93, no. 9, pp. 2539–2542, Sep. 2013.
[19] Z. Zheng, T. Yang, W.-Q. Wang, and H. C. So, "Robust adaptive beamforming via simplified interference power estimation," *IEEE Trans. Aerosp. Electron. Syst.*, vol. 55, no. 6, pp. 3139–3152, Dec. 2019.
[20] Y. Gu, N. A. Goodman, S. Hong, and Y. Li, "Robust adaptive beamforming based on interference covariance matrix sparse reconstruction," *Signal Process.*, vol. 96, no. 5, pp. 375–381, 2014.
[21] Z. Zheng, W.-Q. Wang, H. C. So, and Y. Liao, "Robust adaptive beamforming using a novel signal power estimation algorithm," *Digit. Signal Process.*, vol. 95, Dec. 2019, Art. no. 102574.
[22] X. Zhu, X. Xu, and Z. Ye, "Robust adaptive beamforming via subspace for interference covariance matrix reconstruction," *Signal Process.*, vol. 167, Feb. 2020, Art. no. 107289.
[23] Y. Gu and A. Leshem, "Robust adaptive beamforming based on interference covariance matrix reconstruction and steering vector estimation," *IEEE Trans. Signal Process.*, vol. 60, no. 7, pp. 3881–3885, Jul. 2012.
[24] S. Sun and Z. Ye, "Robust adaptive beamforming based on a method for steering vector estimation and interference covariance matrix reconstruction," *Signal Process.*, vol. 182, May 2021, Art. no. 107939.
[25] A. De Maio, L. Pallotta, J. Li, and P. Stoica, "Loading factor estimation under affine constraints on the covariance eigenvalues with application to radar target detection," *IEEE Trans. Aerosp. Electron. Syst.*, vol. 55, no. 3, pp. 1269–1283, Jun. 2019.
[26] L. Du, J. Li, and P. Stoica, "Fully automatic computation of diagonal loading levels for robust adaptive beamforming," *IEEE Trans. Aerosp. Electron. Syst.*, vol. 46, no. 1, pp. 449–458, Jan. 2010.
[27] R. O. Schmidt, "Multiple emitter location and signal parameter estimation," *IEEE Trans. Antennas Propag.*, vol. 34, no. 3, pp. 276–280, Mar. 1986.
[28] J. Capon, "High-resolution frequency-wavenumber spectrum analysis," *Proc. IEEE*, vol. 57, no. 8, pp. 1408–1418, Aug. 1969.
[29] P. P. Vaidyanathan and P. Pal, "Sparse sensing with co-prime samplers and arrays," *IEEE Trans. Signal Process.*, vol. 59, no. 2, pp. 573–586, Feb. 2011.
[30] F. Dong, W. Wang, and B. Wang, "DoA estimation and sensors self-calibration for partially calibrated array," in *Proc. IEEE Oceans*, Biloxi, MS, USA, Oct. 2020, pp. 1–5.
[31] Z. Wang, Z. Yang, S. Wu, H. Li, S. Tian, and X. Chen, "An improved multiple signal classification for nonuniform sampling in blade tip timing," *IEEE Trans. Instrum. Meas.*, vol. 69, no. 10, pp. 7941–7952, Oct. 2020.
[32] F. Huang, W. Sheng, and X. Ma, "Modified projection approach for robust adaptive array beamforming," *Signal Process.*, vol. 92, no. 7, pp. 1758–1763, Jul. 2012.
[33] M. Zhang, X. Chen, and A. Zhang, "A simple tridiagonal loading method for robust adaptive beamforming," *Signal Process.*, vol. 157, pp. 103–107, Apr. 2019.
[34] R. Roy and T. Kailath, "Esprit-estimation of signal parameters via rotational invariance techniques," *IEEE Trans. Acoust., Speech, Signal Process.*, vol. 37, no. 7, pp. 984–995, Jul. 1989.
[35] S. Marcos, A. Marsal, and M. Benidir, "The propagator method for source bearing estimation," *Signal Process.*, vol. 42, pp. 121–138, Mar. 1995.
[36] J. Chen, Y. Wu, H. Cao, and H. Wang, "Fast algorithm for DOA estimation with partial covariance matrix and without eigendecomposition," *J. Signal Inf. Process.*, vol. 2, no. 4, pp. 266–269, 2011.
[37] S. Mohammadzadeh, V. H. Nascimento, R. C. de Lamare, and O. Kukrer, "Maximum entropy-based interference-plus-noise covariance matrix reconstruction for robust adaptive beamforming," *IEEE Signal Process. Lett.*, vol. 27, pp. 845–849, 2020.
[38] I. S. Reed, J. D. Mallett, and L. E. Brennan, "Rapid convergence rate in adaptive arrays," *IEEE Trans. Aerosp. Electron. Syst.*, vol. AES-10, no. 6, pp. 853–863, Nov. 1974.
[39] M. Grant, S. Boyd, and Y. Ye. (2009). *CVX: MATLAB Software for Disciplined Convex Programming*. [Online]. Available: http://cvxr.com/cvx/
[40] O. Besson and P. Stoica, "Decoupled estimation of DOA and angular spread for a spatially distributed source," *IEEE Trans. Signal Process.*, vol. 48, no. 7, pp. 1872–1882, Jul. 2000.
[41] S. Shahbazpanahi, A. B. Gershman, Z.-Q. Luo, and K. M. Wong, "Robust adaptive beamforming for general-rank signal models," *IEEE Trans. Signal Process.*, vol. 51, no. 9, pp. 2257–2269, Sep. 2003.

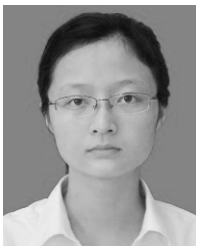

LIN CHANG received the B.S. degree in electronic information science and technology and the M.S. degree in signal and information processing from the Ocean University of China, Qingdao, China, in 2014 and 2015, respectively, where she is currently pursuing the Ph.D. degree. Her research interests include signal enhancement, adaptive array signal processing, and signal recognition.

HUA YANG received the M.S. degree from Shandong University and the Ph.D. degree from Shanghai Jiao Tong University, Shanghai, China. She is currently a Professor with the Information Science and Engineering College, Ocean University of China, Qingdao, China. She also works as a Principal Investigator of the National Natural Science Foundation of China. Her research interests include wireless signal modeling and recognition, and the development of electronic products and systems.

T. AARON GULLIVER (Senior Member, IEEE) received the Ph.D. degree in electrical engineering from the University of Victoria, Victoria, BC, Canada, in 1989. From 1989 to 1991, he was employed as a Defence Scientist with Defence Research Establishment Ottawa, Ottawa, ON, Canada. He has held academic positions at Carleton University, Ottawa, and the University of Canterbury, Christchurch, New Zealand. He joined the University of Victoria, in 1999, where he is currently a Professor with the Department of Electrical and Computer Engineering. His research interests include information theory and communication theory, cryptography and security, and signal processing for communication systems. In 2002, he became a fellow of the Engineering Institute of Canada, and a fellow of the Canadian Academy of Engineering, in 2012.

SHIZHE TAN received the B.S. and M.S. degrees in mechanical and electronic engineering from the University of Shandong, in 1996, and the Ph.D. degree in mechanical engineering from Shanghai Jiao Tong University, Shanghai, China, in 2002. From 2002 to 2005, he was a Postdoctoral Researcher with the Robot Laboratory, Harbin Institute of Technology. Since 2005, he has been an Assistant Professor with the Electronic Engineering Department, Ocean University of China. His research interests include underwater sensors and applications.

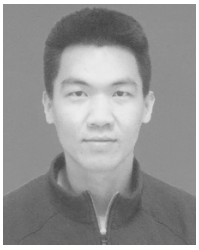

YAN WANG received the B.S. degree from the College of Information Science and Engineering, Jinan University, Jinan, in 2004, and the M.S. and Ph.D. degrees from the College of Information Science and Engineering, Ocean University of China, Qingdao, in 2008 and 2020, respectively. He is currently a Lecturer with the School of Physics and Electronic Engineering, Taishan University. His research interests include wireless communication systems, underwater acoustic communication systems, and UWB systems.